Bioorganic & Medicinal Chemistry Letters 22 (2012) 912–915

Contents lists available at SciVerse ScienceDirect

Bioorganic & Medicinal Chemistry Letters

journal homepage: www.elsevier.com/locate/bmcl

Pyrazolopyridine inhibitors of B-Raf^{V600E}. Part 3: An increase in aqueous solubility via the disruption of crystal packing

Steve Wenglowsky [a], David Moreno [a,*], Joachim Rudolph [b], Yingqing Ran [b], Kateri A. Ahrendt [a], Alisha Arrigo [a], Ben Colson [a], Susan L. Gloor [a], Gregg Hastings [a]

[a] Array BioPharma, 3200 Walnut Street, Boulder, CO 80301, United States
[b] Genentech, Inc., 1 DNA Way, South San Francisco, CA 94080-4990, United States

ARTICLE INFO

Article history:
Received 8 November 2011
Revised 1 December 2011
Accepted 5 December 2011
Available online 10 December 2011

Keywords:
B-Raf^{V600E}
Aqueous solubility
Single-crystal X-ray
Crystal packing
Crystal lattice energy

ABSTRACT

A single crystal was obtained of a lead B-Raf^{V600E} inhibitor with low aqueous solubility. The X-ray crystal structure revealed hydrogen-bonded head-to-tail dimers formed by the pyrazolopyridine and sulfonamide groups of a pair of molecules. This observation suggested a medicinal chemistry strategy to disrupt crystal packing and reduce the high crystal lattice energy of alternative inhibitors. Both a bulkier group at the interface of the dimer and an out-of-plane substituent were required to decrease the compound's melting point and increase aqueous solubility. These substituents were selected based on previously developed structure–activity relationships so as to concurrently maintain good enzymatic and cellular activity against B-Raf^{V600E}.

Our laboratory has recently disclosed a series of ATP-competitive B-Raf^{V600E} inhibitors which utilized 3-methoxy pyrazolopyridine as a novel hinge-binding group.[1,2] Optimization led to compounds **1** and **2**, potent and selective inhibitors of B-Raf^{V600E}, which were highly active against a broad panel of melanoma and colon cancer cell lines driven by this activating mutation (Fig. 1). Although compounds **1** and **2** possessed favorable ADME profiles, their aqueous solubility was low (<10 μg/mL at pH 6.5 and 7.4). As a result, oral exposure in mice was best achieved utilizing a solution formulation of 40% PEG400/10% ethanol/50% water. Due to concerns with daily dosing of high concentrations of PEG400 in efficacy and tolerability studies, compounds **1** and **2** were reformulated as amorphous spray-dried dispersions (SDD) on hydroxypropyl methylcellulose acetate succinate (HPMCAS) polymer at 25% loading.[3] The SDD formulation led to oral exposures for these compounds sufficient for significant in vivo anti-tumor efficacy.

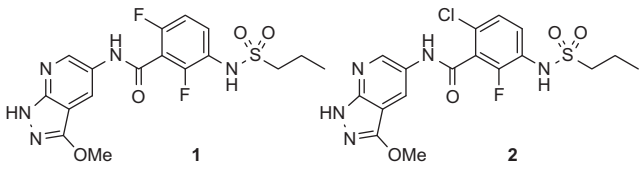

Figure 1. B-Raf^{V600E} inhibitors **1** and **2**.

While SDD formulations offer an approach to improve oral exposure and have been used successfully in the clinic,[4] an additional processing step is required for manufacturing. Another issue is the presence of a large amount of polymer which presents a higher pill burden for the patient. Thus, the development of a potent and efficacious B-Raf^{V600E} inhibitor with an increase in aqueous solubility would be advantageous.

In general, the aqueous solubility of a solute is dependent upon two factors: the ability of the solute to interact with water (lipophilicity) and the crystal lattice energy of the solute.[5] While most of the analogs prepared during the lead optimization of the pyrazolopyridine series fell within a narrow range of lipophilicity (*C*log*P* = 1.43–1.86), a broad range of melting points was observed (MP = 173–261 °C). As predicted by the general solubility equation of Jain and Yalkowsky, in which $\log S = 0.5 - 0.01(\mathrm{MP} - 25) - C\log P$,[5] a wide range of aqueous solubility was likewise observed and correlated with melting point. This broad range of melting points within a series of structurally similar analogs suggests that subtle crystal packing effects exist which are modulated by varying the substituents around the molecule. In an effort to exploit this effect and rationally guide the discovery of a potent B-Raf^{V600E} inhibitor with reduced crystal lattice energy, a single crystal of compound **1** was obtained. Reported herein is the design and synthesis of alternative B-Raf^{V600E} inhibitors which bear substituents that disrupt the observed crystal packing of **1** and lead to compounds with lower melting points and increased aqueous solubility.[6,7]

* Corresponding author.
E-mail address: david.moreno@arraybiopharma.com (D. Moreno).

0960-894X/$ - see front matter © 2011 Elsevier Ltd. All rights reserved.
doi:10.1016/j.bmcl.2011.12.030

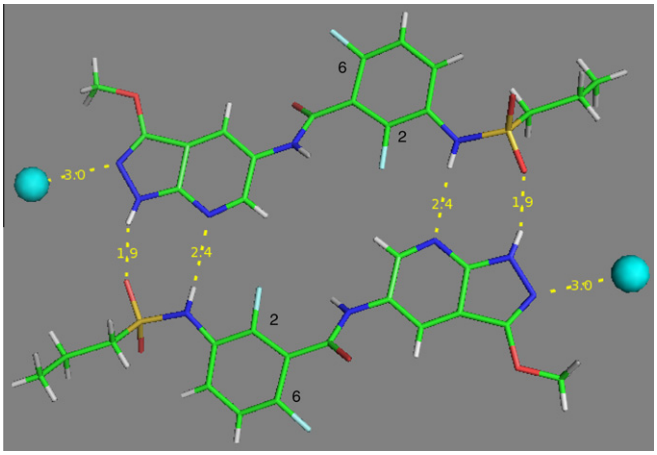

Figure 2. X-ray crystal structure of **1**. Water molecules are represented as blue spheres. Carbon atoms are rendered in green, hydrogen in white, nitrogen in blue, oxygen in red, fluorine in light blue and sulfur in yellow. Hydrogen bonds interactions are illustrated with yellow dashed lines and hydrogen bond distances are given in Angstroms. Numbering around the central phenyl ring is indicated.

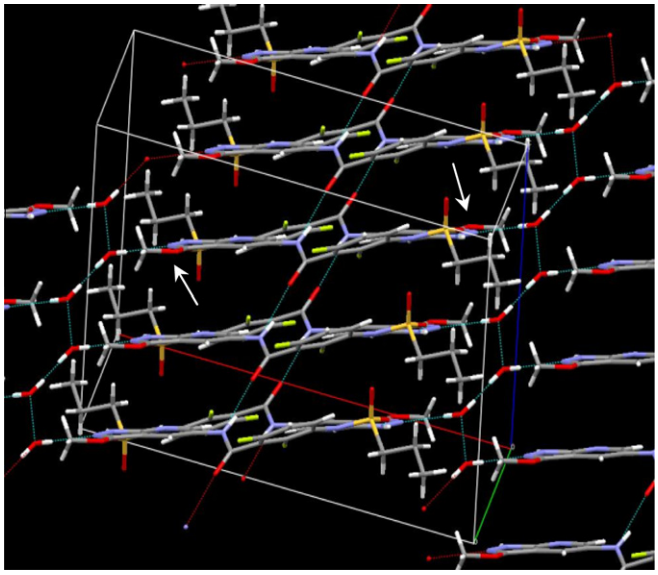

Figure 3. X-ray crystal structure of **1**. Carbon atoms are rendered in gray, hydrogen in white, nitrogen in blue, oxygen in red, and sulfur in yellow. Hydrogen bonds interactions are depicted by cyan dash lines and the unit cell is illustrated. The 3-methoxy substituents of a dimer of **1** are highlighted with white arrows.

Sixteen slow evaporation and sixteen slow diffusion experiments were carried out on **1** in order to prepare suitable material for structure determination by X-ray diffraction.[8] A mixed solvent system of 70:30 EtOH–H_2O provided colorless plates of sufficient size and quality for structure determination.[9] The crystal structure revealed that the monohydrate of compound **1** crystallizes in an extended conformation, an arrangement which leads to the formation of head-to-tail dimers. The donor and acceptor pair of the pyrazolopyridine forms two hydrogen bonds with a donor and acceptor pair of the sulfonamide from another molecule of **1**; this then positions the pyrazolopyridine from the second molecule of **1** to form hydrogen bonds back to the sulfonamide of the first molecule (Fig. 2). The four aromatic rings of the dimer lie in the same plane, while the amide linkers are rotated out of this plane and do not take part in the dimer formation. The presence of four hydrogen bonds between the two molecules of the dimer represents a stable arrangement in the crystalline state, and is likely a common feature of many of the analogs within this series.

Additional analysis of the X-ray crystal structure of **1** revealed that each pyrazolopyridine forms a π-stacking interaction with another pyrazolopyridine both above and below the plane of each dimer. Likewise, the central phenyl rings are in proximity to form π-stacking interactions. In this way, the dimer pairs stack one on top of another (Fig. 3). Due to the rotation of the amides out of the plane of the dimers (Fig. 2), they are aligned to form hydrogen bonds both above and below with the amides from another dimer pair. Thus the π-stacking and hydrogen bonding interactions between the amide linkers reinforce each other and result in the formation of a long-range network of π-stacked dimers. This network appears to be a highly stable arrangement and likely contributes to the high melting point of compound **1** and many of the analogs in this series of B-Raf^{V600E} inhibitors.

These observations led to two hypotheses that could disrupt the crystal packing of an analog of **1** and lead to a compound with a lower melting point and increased aqueous solubility. The first was to destabilize the head-to-tail dimer formation. Since the hydrogen bond donors on the pyrazolopyridine and sulfonamide are critical for binding to B-Raf^{V600E},[1] it would not be possible to destabilize the dimer by blocking either of these groups (by, e.g., methylation) and still maintain potency. An alternative method would be to incorporate a sterically bulky group at the dimer interface proximate to one of the hydrogen bonds. Based on the X-ray crystal structure of **1** bound to B-Raf^{WT} and the structure–activity relationships developed for this series,[2] it was proposed that the incorporation of a chlorine in place of the fluorine at the 2-position of the central phenyl ring would maintain activity against the target while weakening two of the hydrogen bonds of the dimer (Fig. 2). The required 2-Cl, 6-F substitution on this central phenyl ring led to compound **3**.

The second hypothesis that could disrupt the crystal packing of an analog of **1** was to introduce an out-of-plane substituent.[6,10,11] The propensity of the pyrazolopyridine to engage in π-stacking suggested attaching the out-of-plane substituent directly to the heterocycle, and the replacement of the 3-methoxy substituent was proposed (Fig. 3). Previously determined structure–activity relationships revealed that although 3-alkoxy groups on the pyrazolopyridine hinge-binding core provided compounds with the best cellular activity (pERK ⩽ 20 nM), several other 3-substituents provided inhibitors with only a 2- to 4-fold reduction in potency (-Br, -I, -Me, -Et: pERK = 36–86 nM).[2] Thus, it was proposed that a small, branched group at the 3-position could impart both the desired B-Raf^{V600E} cellular activity and a lower melting point than **1**. This hypothesis led to 3-isopropyl and 3-cyclopropyl pyrazolopyridines **4** and **5**.

As expected, compound **3** was essentially equipotent with **1** and **2** in the enzymatic and cellular assays against B-Raf^{V600E} (Table 1).[12] However, the melting point of **3** was nearly identical to **1** (221 vs 229 °C) suggesting that the substitution of chlorine for fluorine at the 2-position of the central phenyl ring was insufficient to disrupt head-to-tail dimer formation. Given that the *C*log*P* of **3** was also similar to both **1** and **2**, no improvement in aqueous solubility was expected which was verified experimentally.[13]

Compounds **4** and **5** were prepared next via established synthetic methods.[1] 3-Isopropyl substituted pyrazolopyridine **4** (B-Raf^{V600E} = 14 nM, pERK = 89 nM, Table 1) was equipotent to previously prepared 3-methyl (B-Raf^{V600E} = 12 nM, pERK = 86 nM) and 3-ethyl (B-Raf^{V600E} = 9.2 nM, pERK = 84 nM) pyrazolopyridines.[2] However, these compounds were all >4-fold less active in the cellular assay versus comparator compound **1**. In addition, despite the introduction of the out-of-plane substituent, 3-isopropyl pyrazolopyridine **4** still possessed low aqueous solubility. The 3-cyclopropyl pyrazolopyridine **5**, in contrast to all other alkyl substituents examined, was equipotent to **1**. However, like compound **4**, 3-

Table 1
B-Raf^{V60E} activity, solubility and melting point of compounds **1**–**8**

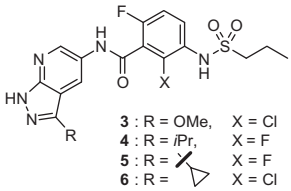

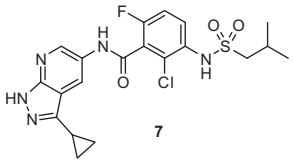

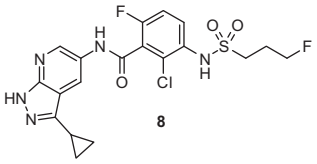

Compound	B-Raf IC_{50}[a] (nm)	pERK IC_{50}[a] (nm)	Sol. pH 6.5, 7.4[b]	MP[c] (°C)	MW	Clog*P*
1	4.8	19	4, 9	229	425	1.61
2	1.7	20	<1, 2	261	442	1.76
3	2.2	19	<1, 2	221	442	1.64
4	14	89	6, n.d.[d]	n.d.[d]	438	2.63
5	2.7	23	1, 4	217	436	2.15
6	3.8	33	54, 127	164	452	2.19
7	2.0	18	1, <1	213	466	2.59
8	0.6	51	130, 265	154	470	1.61

[a] Values are means of at least two experiments.
[b] μg/mL.
[c] MP = melting point of recrystallized material which provided the highest melting polymorph.
[d] n.d. = not determined.

cyclopropyl pyrazolopyridine **5** showed no significant reduction in melting point versus **1** (217 °C) and similarly poor aqueous solubility.

Although neither the incorporation of a bulky substituent at the dimer interface nor an out-of-plane substituent at the pyrazolopyridine 3-position was sufficient to induce an increase in aqueous solubility, it seemed prudent to apply both of these hypotheses to the same molecule. This strategy led to B-Raf^{V600E} inhibitor **6**.

The cellular activity of compound **6** (pERK = 33 nM) was within twofold of compounds **1**–**3** and **5**. Furthermore, the melting point of **6** (164 °C) was >50 °C lower than these inhibitors indicating that the crystal lattice energy of **1** was significantly reduced. Despite the increase in lipophilicity resulting from the replacement of the methoxy group with a cyclopropyl group, the aqueous solubility of **6** nonetheless increased >10-fold versus **1**, and was >50-fold greater than **2** and **3** (Table 1). A recrystallization screen with over 10 solvent systems failed to produce a crystal with a higher melting point. Differential scanning calorimetry (DSC) confirmed the melting point of 164 °C and indicated a second polymorph melting at 140 °C.

A single crystal of **6** was obtained to account for its low melting point.[14] The X-ray structure revealed no head-to-tail dimer formation which led to fewer π-stacking interactions than for **1** (Fig. 4). The inability of **6** to form head-to-tail dimers results from the conformation of the central phenyl ring. While compound **6** also resides in an extended conformation, the bond from the amide carbonyl to the central phenyl ring is rotated approximately 180° compared to **1** rendering dimer formation impossible (Fig. 5). As such, the hydrogen bonds of compound **6** must be satisfied via an alternative arrangement in the solid state, leading to reduced crystal lattice energy, decreased melting point and higher aqueous solubility. The substitution of 3-cyclopropyl for 3-methoxy on the pyrazolopyridine must be required to achieve this alternative conformation since the melting point and low aqueous solubility of **3** suggests a similar crystal lattice formation to **1**. Since compound **6** possesses higher molecular weight than compounds **1**–**5**, and greater lipophilicity than compounds **1**–**3**, crystal packing must play the predominant role in determining its aqueous solubility.

It was of interest to know whether the increase in aqueous solubility observed for **6** would translate to related compounds bearing sulfonamide tails other than propyl. Previously determined structure–activity relationships revealed two propyl replacements with similar activity, isobutyl and 3-fluoropropyl.[2] Incorporation of these groups at the sulfonamide of **6** led to compounds **7** and **8**.

The cellular activity of isobutyl sulfonamide **7** was excellent (pERK = 18 nM), yet the inclusion of this single methyl group on the molecule led to a significant increase in melting point and a complete erosion of the increased aqueous solubility seen with **6**. This result was unexpected since additional branching was expected to maintain or even further increase aqueous solubility, yet the melting point indicates this compound is still able to adopt some highly stable arrangement in the crystalline state. In contrast, the melting point and aqueous solubility of compound **8** suggests the formation of a similar crystalline polymorph to that of **6**. The addition of the 3-fluoro group to the propyl sulfonamide tail of **6**

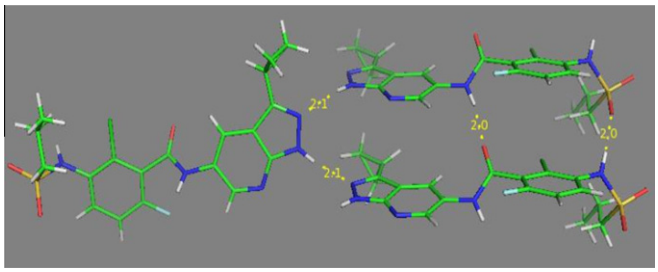

Figure 4. X-ray crystal structure of **6**. Carbon atoms are rendered in green, hydrogen in white, nitrogen in blue, oxygen in red, fluorine in light blue and sulfur in yellow. Hydrogen bond interactions are illustrated with yellow dashed lines and hydrogen bond distances are given in Angstroms.

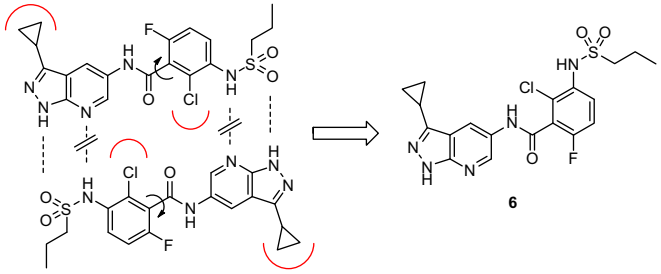

Figure 5. Conformation change of **6** due to the incorporation of sterically demanding substituents.

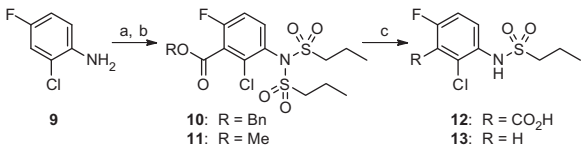

Scheme 1. Reagents and conditions: (a) 1.05 equiv, *n*-BuLi, THF, −78 °C, 1,2-bis(chlorodimethylsilyl)ethane, 1 h, then 1.05 equiv, *n*-BuLi, −78 °C to 22 °C, 1 h, then 1.05 equiv, *n*-BuLi, R-chloroformate, −78 °C, 1 h, 85% for R = Bn, 88% for R = Me; (b) propane-1-sulfonyl chloride, TEA, DCM, 22 °C, 1 h, 82% for **10**, 86% for **11**; (c) aq hydroxide, 4:1 THF/MeOH.

reduces the melting point further to 154 °C and increases the aqueous solubility over **6** by twofold. While the cellular activity of compound **8** was attenuated, it was still within threefold of compound **1**. Compared to compound **2**, the melting point of compounds **6** and **8** were 100 °C less and resulted from only minor structural changes.

The synthesis of the requisite 2-chloro-6-fluoro-3-(propylsulfonamido)benzoic acid **12** initially followed the route used to prepare the regioisomeric 6-chloro-2-fluoro-3-(propylsulfonamido)benzoic acid (Scheme 1).[1] In one step, 2-chloro-4-fluoro aniline **9** was protected with 1,2-bis(chlorodimethylsilyl)ethane, metalated and acylated with benzyl chloroformate. Under aqueous workup conditions the bis-silyl amine was deprotected, and the resulting aniline was bis-sulfonylated to give **10**. However, although the regioisomer of **10**, where the chloro and fluoro substituents were reversed, underwent ester hydrolysis with aqueous KOH at 80 °C, the benzyl ester **10** provided no trace of acid **12** under these conditions. More forcing hydrolysis conditions, with aqueous $Ba(OH)_2$ at 80 °C, provided the desired acid **12**; unfortunately, these conditions led to concomitant decarboxylation leading to **13**. Ultimately, a facile hydrolysis that provided **12** cleanly was obtained via the methyl ester **11**. Hydrolysis with KOH at 80 °C for 16 h provided compound **12** in 58% yield with no trace of decarboxylation. Acid **12** was then coupled to the appropriate anilines under the standard conditions to provide the desired inhibitors.[1]

In summary, potent B-Raf^{V600E} inhibitors with improved aqueous solubility were prepared. A single crystal X-ray of lead compound **1** was obtained, and a medicinal chemistry strategy was developed to disrupt its observed crystal packing. The combination of both an out-of-plane substituent and a bulky group at the interface of the dimer of **1** led to compounds **6** and **8**. It was found that both changes were required to decrease crystal lattice energy resulting in a substantial reduction in melting point. As predicted by the general solubility equation, a significant increase in the aqueous solubility of these two compounds was observed.

Acknowledgements

The authors thank Jaroslaw Mazurek from Avantium for determination of the crystal structure of **1** and Antonio DiPasquale from The University of California, Berkeley for determination of the crystal structure of **6**. The authors also thank Kevin Hunt, Yvan LeHuerou, Li Ren, Stephen Schlachter, and Tony Tang for helpful discussions and support.

References and notes

1. Wenglowsky, S.; Ren, L.; Ahrendt, K. A.; Laird, E. R.; Aliagas, I.; Alicke, B.; Buckmelter, A. J.; Choo, E. F.; Dinkel, V.; Feng, B.; Gloor, S. L.; Gould, S. E.; Gross, S.; Gunzner-Toste, J.; Hansen, J. D.; Hatzivassiliou, G.; Liu, B.; Malesky, K.; Mathieu, S.; Newhouse, B.; Raddatz, N. J.; Ran, Y.; Rana, S.; Randolph, N.; Risom, T.; Rudolph, J.; Savage, S.; Selby, L. T.; Shrag, M.; Song, K.; Sturgis, H. L.; Voegtli, W. C.; Wen, Z.; Willis, B. S.; Woessner, R. D.; Wu, W. –I.; Young, W. B.; Grina, J. *ACS Med. Chem. Lett.* **2011**, *2*, 342.
2. Wenglowsky, S.; Ahrendt, K.; Buckmelter, A. J.; Feng, B.; Gloor, S. L.; Gradl, S.; Grina, J.; Hansen, J. D.; Laird, E. R.; Lunghofer, P.; Mathieu, S.; Moreno, D.; Newhouse, B.; Ren, L.; Risom, T.; Rudolph, J.; Seo, J.; Sturgis, H. L.; Voegtli, W. C.; Wen, Z. *Biorg. Med. Chem. Lett.* **2011**, 5533.
3. Friesen, D. T.; Shanker, R.; Crew, M.; Smithey, D. T.; Curatolo, W. J.; Nightingale, J. A. S. *Mol. Pharm.* **2008**, *5*, 1003.
4. Bollag, G.; Hirth, P.; Tsai, J.; Zhang, J.; Ibrahim, P. N.; Cho, H.; Spevak, W.; Zhang, C.; Zhang, Y.; Habets, G.; Burton, E. A.; Wong, B.; Tsang, G.; West, B. L.; Powell, B.; Shellooe, R.; Marimuthu, A.; Nguyen, H.; Zhang, K. Y. J.; Artis, D. R.; Schlessinger, J.; Su, F.; Higgins, B.; Iyer, R.; D'Andrea, K.; Koehler, A.; Stumm, M.; Lin, P. S.; Lee, R. J.; Grippo, J.; Puzanov, I.; Kim, K. B.; Ribas, A.; McArthur, G. A.; Sosman, J. A.; Chapman, P. B.; Flaherty, K. T.; Xu, X.; Nathanson, K. L.; Nolop, K. *Nature* **2010**, *467*, 596.
5. Jain, N.; Yalkowsky, S. H. *J. Pharm. Sci.* **2001**, *90*, 234.
6. Examples of increasing aqueous solubility by the disruption of molecular planarity: (a) Fray, M. J. *J. Med. Chem.* **2001**, *44*, 1951; (b) Lanier, M. C.; Moorjani, M.; Luo, Z.; Chen, Y.; Lin, E.; Tellew, J. E.; Zhang, X.; Williams, J. P.; Gross, R. S.; Lechner, S. M.; Markison, S.; Joswig, T.; Kargo, W.; Piercey, J.; Santon, M.; Malany, S.; Zhao, M.; Petroski, R.; Crespo, M. I.; Diaz, J. –L.; Saunders, J.; Wen, J.; O'Brien, Z.; Jalali, K.; Madan, A.; Slee, D. H. *J. Med. Chem.* **2009**, *52*, 709; (c) Fujita, Y.; Yonehara, M.; Tetsuhashi, M.; Noguchi-Yachide, T.; Hashimoto, Y.; Ishikawa, M. *Bioorg. Med. Chem. Lett.* **2010**, *18*, 1194.
7. Our laboratory has pursued an additional successful method to disrupt the observed crystal packing of this series which provided an alternative series of B-Raf^{V600E} inhibitors with lowered melting point and improved aqueous solubility: Ren, L.; Laird, E. R.; Buckmelter, A. J.; Dinkel, V.; Gloor, S. L.; Grina, J.; Newhouse, B.; Rasor, K.; Hastings, G.; Gradl, S. N.; Rudolph, J. *Bioorg. Med. Chem. Lett.* doi: 10.1016/j.bmcl.2011.11.092.
8. Slow evaporation procedure: 15–20 mg of compound **1** were added to 16 separate 8 mL vials and to each was added the solvent or mixture of solvents at room temperature until dissolution was observed. Vials were heated to 50–75 °C as required for dissolution. The vials were closed and a small hole was pierced in the cap, and the vials were left at room temperature until crystallization occurred. Vapor diffusion procedure: 15–20 mg of compound **1** were added to 16 separate 16 mL vials; to 8 of the vials was added 8.2 mL of EtOH, while to the other 8 vials 8.2 mL of MeOH was added. Each vial was placed into a 20 mL vial containing a polar or highly non-polar antisolvent. The 20 mL vials were closed and left at room temperature until crystallization occurred.
9. Crystal structure determination of **1** was made by Avantium Technologies BV. The single crystal measurements were performed on a Nonius Kappa-CCD diffractometer equipped with an Oxford Cryostream Liquid Nitrogen Cooler using Mo K_α radiation. The data were collected at 293 and 120 K. The full sphere data were collected up to $\theta = 32.5°$ (17219 reflections) at 120 K and up to $\theta = 27.5°$ (1919 reflections) at 293 K. Data reduction was performed using HKL Scalepack from 8712 reflections within θ range 2–32°. The structure was solved using direct methods by SHELX-97. The structure was refined by least square full matrix refinement using SHELX-97. All H-atoms were found on the Fourier difference map and refined isotropically. The absolute configuration was determined using Flack parameters based on anomalous dispersion effect. Crystal data and structure refinement for **1**: $C_{17}H_{17}F_2N_5O_4S{\cdot}H_2O$, monoclinic, space group: P 2_1/C, $a = 18.936(3)$ Å, $b = 5.114(2)$ Å, $c = 19.549(3)$ Å, $\beta = 93.777(9)°$, $V = 1889.0(8)$ Å^3, $Z = 4$, $D_c = 1.559$ g/cm^3, $\mu = 0.234$, $F(000) = 920$, crystal size = 0.55 × 0.30 × 0.05 mm, $R_1 = 0.0665$, $R_{int} = 0.0402$ based on 6770 independent reflections.
10. Lovering, F.; Bikker, J.; Humblet, C. *J. Med. Chem.* **2009**, *52*, 6752.
11. Hashimoto, Y.; Ishikawa, M. *J. Med. Chem.* **2011**, *54*, 1539.
12. Inhibitor enzymatic activity was determined utilizing full-length B-Raf^{V600E}. Inhibition of basal ERK phosphorylation in Malme-3M cells was used as the mechanistic cellular assay and to drive the structure–activity relationships. For complete experimental details regarding the enzymatic and mechanistic cellular screening assays, please refer to Ref. 1.
13. For complete experimental details regarding aqueous solubility determinations, please refer to Ref. 1.
14. Crystal structure determination of **6** was made by the University of California, Berkeley, College of Chemistry, X-ray Crystallography Facility. Compound **6** was recrystallized from isopropyl ether. A colorless rod 0.15 × 0.12 × 0.08 mm in size was mounted on a Cryoloop with Paratone oil. Data were collected in a nitrogen gas stream at 200(2) K using phi and omega scans. Crystal-to-detector distance was 60 mm and exposure time was 10 s per frame using a scan width of 1.0°. Data collection was 97.4% complete to 67.00° in θ. A total of 14251 reflections were collected covering the indices, $-46 \leqslant h \leqslant 46$, $-6 \leqslant k \leqslant 4$, $-34 \leqslant l \leqslant 34$. 4271 reflections were found to be symmetry independent, with an R_{int} of 0.0542. Indexing and unit cell refinement indicated a C-centered, monoclinic lattice. The space group was found to be C2/c (No. 15). The data were integrated using the Bruker SAINT software program and scaled using the SADABS software program. Solution by direct methods (SIR-2004) produced a complete heavy-atom phasing model consistent with the proposed structure. All non-hydrogen atoms were refined anisotropically by full-matrix least-squares (SHELXL-97). All hydrogen atoms were placed using a riding model. Their positions were constrained relative to their parent atom using the appropriate HFIX command in SHELXL-97. Crystal data and structure refinement for **6**: $C_{44}H_{52}Cl_2F_2N_{10}O_7S_2$, monoclinic, space group: C2/c, $a = 39.3619(13)$ Å, $b = 4.9943(2)$ Å, $c = 29.1556(11)$ Å, $\beta = 122.351(2)°$, $V = 4841.9(3)$ Å^3, $Z = 4$, $D_c = 1.380$ g/cm^3, $\mu = 0.2583$, $F(000) = 2104$, crystal size = 0.15 × 0.12 × 0.08 mm^3, $R_1 = 0.0642$, $R_{int} = 0.0542$ based on 4271 independent reflections.